Eur. Phys. J. B **21**, 135–144 (2001)

THE EUROPEAN PHYSICAL JOURNAL B

EDP Sciences

Finite-size effects with rigid boundaries on nonequilibrium fluctuations in a liquid

J.M. Ortiz de Zárate[a] and L. Muñoz Redondo

Dpto. Física Aplicada 1, Facultad de CC. Físicas, Universidad Complutense, 28040 Madrid, Spain

Received 2 November 2000

Abstract. In a recent publication [Physica A **291**, 113 (2001)] the static structure factor of a liquid in a thermal nonequilibrium state was calculated exactly from the random Boussinesq equations, in the absence of convection, for "stress-free" boundary conditions. In the present paper we present a similar calculation, but with the more realistic "no-slip" boundary conditions. In this case an explicit calculation cannot be performed and we use a zeroth-order Galerkin approximation. The main conclusion is that the approximate structure factor thus calculated has qualitative the same behavior as the exact result for "stress-free" boundary conditions. The typical divergence on q^{-4} of the nonequilibrium part of the structure factor crosses over to a q^2 dependence for extremely small wavevectors q. Separating both behaviors a maximum appears indicating that fluctuations with a particular wavevector, $q_{\max}$, are maximally enhanced.

PACS. 05.40.-a Fluctuation phenomena, random processes, noise, and Brownian motion – 47.54.+r Pattern selection; pattern formation – 78.35.+c Brillouin and Rayleigh scattering; other light scattering

1 Introduction and motivation

During the past years considerable effort has been devoted to the study of hydrodynamic fluctuations in liquids in stationary thermal nonequilibrium states, particularly when a liquid layer is subjected to a constant temperature gradient, ∇T_0. It turns out that density or temperature fluctuations in such nonequilibrium states become spatially long-ranged, even in the absence of any convective instabilities [1].

The long-range nature of the fluctuations manifests itself as a wavevector-dependent enhancement in the Rayleigh component of the structure factor. The structure factor, $S(q)$, can be measured experimentally, because it is proportional to the intensity of light scattered by the liquid. As originally predicted by mode-coupling theory [2] and later confirmed by fluctuating hydrodynamics [3–6], $S(q)$ depends on the fluctuations wavevector q, for small scattering angles, as:

$$S(q) = \rho^2 \kappa_T k_{\mathrm{B}} T \frac{\gamma - 1}{\gamma} \left[1 + \frac{(c_P/T)(\nabla T_0)^2}{D_T^2 (P+1)} \frac{1}{q^4} \right], \quad (1)$$

where ρ is the density, κ_T the isothermal compressibility, c_P the isobaric specific heat capacity, γ the heat-capacity ratio, D_T the thermal diffusivity and P the Prandtl number of the liquid. The symbol k_{B} represents Boltzmann's constant and T the average temperature in the fluid layer. We note that $S(q)$, as given by (1), contains an equilibrium contribution and a nonequilibrium enhancement.

The equilibrium contribution S_{E} is obtained by taking $\nabla T_0 = 0$ in (1), so that $S_{\mathrm{E}} = \rho^2 \kappa_T k_{\mathrm{B}} T[(\gamma - 1)/\gamma]$. The resulting S_{E} is independent of the wavevector q and equals the traditional formula for the isotropic Rayleigh-scattering intensity [7].

The nonequilibrium enhancement is proportional to the square of the temperature gradient and diverges as q^{-4} for $q \to 0$. The dependence on q^{-4} means that to observe any nonequilibrium enhancement, the scattering intensity has to be measured at small angles. This q^{-4} dependence of the intensity of scattered light has been confirmed by several small-angle Rayleigh-scattering experiments [8–10].

The divergence of the structure factor as q^{-4} cannot go on indefinitely up to wave numbers corresponding to macroscopic wavelengths. Specifically two sources can be identified that will cause deviations from the q^{-4} behavior at very small wavevectors. Firstly, gravity causes the q^{-4} divergence to be quenched, the structure factor reaching a constant limit in $q \to 0$, as elucidated by Segrè *et al.* [11,12]. This gravitationally induced saturation of the q^{-4} divergence has been confirmed by Vailati and Giglio [13,14] in ultra-low-angle light-scattering experiments. Secondly, as a constant temperature gradient has to be applied to a liquid layer with a finite height, finite-size effects are expected to cause also a deviation from the q^{-4} behavior at small angles. These finite-size effects have been considered explicitly only very recently [15].

[a] e-mail: fiap102@sis.ucm.es

In [15] the finite-size effects were accounted for by solving the fluctuating hydrodynamics equations in the Boussinesq approximation, subjected to boundary conditions. The Boussinesq approximation is equivalent to assuming that density fluctuations are caused by temperature fluctuations, while neglecting pressure fluctuations. Consequently, Boussinesq approximation can be used for evaluating the Rayleigh component of the scattering spectrum, since pressure fluctuations only affect the Brillouin components. It is for the Rayleigh component of the scattering spectrum for which accurate experimental information on nonequilibrium fluctuations has been obtained [8–10,13,14]. The main conclusion reached in [15] is that in the nonequilibrium contribution to the Rayleigh-scattering intensity finite-size effects cause a crossover from the q^{-4} divergence to a q^2 dependence valid for extremely small scattering wavevectors. The crossover from q^{-4} to q^2 means that a maximum in the scattering intensity appears. The position of the maximum is of the order of the inverse of the finite height of the system. The existence of this maximum indicates that fluctuations with a particular wavevector are maximally enhanced. Hence, the nonequilibrium effects couple with the finite size of the system to select a particular length scale, for which the nonequilibrium fluctuations are maximally enhanced.

The actual results obtained from the analysis of finite-size effects will depend on the boundary conditions considered. Ortiz de Zárate *et al.* [15] considered "stress-free" boundary conditions for the fluctuating velocity because of their mathematical simplicity. But these conditions correspond to a fluid bounded by two free surfaces, which is a rather unrealistic case [16]. For the realistic case of a fluid bounded by two rigid solid plates the adequate boundary conditions are "no-slip" boundary conditions [16]. The main goal of the present paper is to analyze finite-size effects in the scattered intensity, as in [15], with the more realistic "no-slip" boundary conditions. Other investigators have also studied finite-size effects on nonequilibrium fluctuations, using both "stress-free" and "no-slip" boundary conditions, but they always have focusing on the situation close to the convective instability [17–21]. Actually, they considered the influence of thermal noise at the convective instability and studied the divergence in $S(q)$ as the critical Rayleigh number is approached. We are considering here the same problem but in a different limit, namely when gravity is negligible and the system is in a quiescent stable state. Malek Mansour *et al.* [22,23] have considered the effects of boundary conditions on some correlation functions in a fluid subjected to a stationary temperature gradient. But they adopted hydrodynamic simplifications appropriate to Brillouin scattering, while we are here concerned with Rayleigh scattering. Bena *et al.* have recently reported results of finite-size effects on nonequilibrium fluctuations in Kolmogorov flow [24]. Again as a consequence of the hydrodynamic simplifications adopted, they did not consider the Rayleigh component of the scattering spectrum.

The following material is organized in five sections. In Section 2, we present the linearized Boussinesq equations supplemented with random noise terms, which are the starting point of the analysis. In Section 3, for the sake of completeness and for subsequent comparison, we review the results of [15] for two free boundaries, and we briefly sketch how they were obtained. Section 4 contains the main results of the present paper, where we consider two rigid boundaries and adopt an approximate Galerkin method to solve the linearized random Boussinesq equations. In Section 5 we present a detailed analysis of the finite-size effects as they appear in low-angle light-scattering experiments, comparing the results with "stress-free" and with "no-slip" boundary conditions. Our conclusions are summarized in Section 6.

2 The linearized random Boussinesq equations

We consider a liquid layer bounded between two horizontal planes separated by a distance L. The liquid layer is subjected to a stationary temperature gradient, ∇T_0, in the direction of the Z-axis. This temperature gradient is established by maintaining the two horizontal planes at different temperatures. The size of the system in the XY plane is assumed to be much larger than the size L of the system in the Z-direction.

To calculate the structure factor of the fluid in this situation, we use the Boussinesq equations which we supplement with a random current tensor $\delta\mathsf{T}(\mathbf{r},t)$ and a random heat flow $\delta\mathbf{Q}(\mathbf{r},t)$. This procedure was first employed by Swift and Hohenberg to study the influence of noise close to the first convective instability [17]. This has been further developed by many authors, but always focusing on the situation close to the convective instability [18–21]. As mentioned in Section 1, to focus on the finite-size effects, we consider here the limit of negligible gravity, thus $g \to 0$. For this particular case, the quiescent state is always stable. To describe fluctuations around this stable state we use the linearized Boussinesq equations without the buoyancy term [16,25]:

$$\frac{\partial}{\partial t}(\nabla^2 w) = \nu\nabla^2(\nabla^2 w) + \frac{1}{\rho}\left\{\nabla\times[\nabla\times(\nabla\cdot\delta\mathsf{T})]\right\}_z \quad (2a)$$

$$\frac{\partial\theta}{\partial t} = D_T\ \nabla^2\theta - \nabla T_0\ w - \frac{D_T}{\lambda}\nabla\cdot\delta\mathbf{Q}, \quad (2b)$$

where, in the notation of Chandrasekhar [16], $\theta(\mathbf{r},t)$ are the local fluctuations in the temperature ($\theta = \delta T$), and $w(\mathbf{r},t)$ are the local fluctuations in the Z-component of the velocity ($w = \delta v_z$). The symbol ν represents the kinematic viscosity and λ the thermal conductivity of the liquid. Note that in the Boussinesq approximation the liquid is incompressible [16,25], so that D_T can be identified with the thermal diffusivity $\lambda/(\rho\ c_P)$. In writing equation (2) we have assumed that the thermophysical properties of the fluid depend weakly on temperature, so that the variation of these properties along the Z-direction can be neglected. In practice, this is a very good approximation [26]. Equation (2a) is obtained by taking a double curl in the velocity fluctuations equation, so as to eliminate the pressure gradient [16].

$$\begin{pmatrix} F_1(\omega,\mathbf{q}_\parallel,z) \\ F_2(\omega,\mathbf{q}_\parallel,z) \end{pmatrix} = \begin{pmatrix} \frac{\mathrm{i}}{\rho}\left\{ \begin{array}{l} \frac{\mathrm{d}^2}{\mathrm{d}z^2}(q_x\delta\hat{T}_{zx}+q_y\delta\hat{T}_{zy})+q_\parallel^2(q_x\delta\hat{T}_{xz}+q_y\delta\hat{T}_{yz}) \\ -\mathrm{i}\frac{\mathrm{d}}{\mathrm{d}z}\left[q_\parallel^2\delta\hat{T}_{zz}-\left(q_x^2\delta\hat{T}_{xx}+q_y^2\delta\hat{T}_{yy}+q_xq_y(\delta\hat{T}_{xy}+\delta\hat{T}_{yx})\right)\right] \end{array} \right\} \\ -\frac{D_T}{\lambda}\left[\mathrm{i}(q_x\delta\hat{Q}_x+q_y\delta\hat{Q}_y)+\frac{\mathrm{d}}{\mathrm{d}z}\delta\hat{Q}_z\right] \end{pmatrix}. \tag{4}$$

As in the usual fluctuating hydrodynamics approach, we have supplemented the linearized Boussinesq equations with a random current tensor $\delta\mathsf{T}(\mathbf{r},t)$ and a random heat flow $\delta\mathbf{Q}(\mathbf{r},t)$, to account for the contributions from non-hydrodynamic degrees of freedom which manifest themselves as rapidly varying short-range fluctuations [3–6,21,27,28]. The equilibrium correlation functions between the different components of $\delta\mathsf{T}$ and $\delta\mathbf{Q}$ are known and were first calculated by Landau and Lifshitz [27]. Note that in equation (2a) the subscript z means that the noise term has to be identified with the Z-component of the vector between curly brackets.

To solve the system of stochastic differential equations (2) taking into account boundary conditions in $z=0$ and $z=L$ we apply Fourier transformations in time and in the XY plane, and obtain [15]:

$$\begin{pmatrix} \mathrm{i}\omega\left[\frac{\mathrm{d}^2}{\mathrm{d}z^2}-q_\parallel^2\right]-\nu\ \left[\frac{\mathrm{d}^2}{\mathrm{d}z^2}-q_\parallel^2\right]^2 & 0 \\ \nabla T_0 & \mathrm{i}\omega-D_T\ \left[\frac{\mathrm{d}^2}{\mathrm{d}z^2}-q_\parallel^2\right] \end{pmatrix} \times \begin{pmatrix} w(\omega,\mathbf{q}_\parallel,z) \\ \theta(\omega,\mathbf{q}_\parallel,z) \end{pmatrix} = \begin{pmatrix} F_1(\omega,\mathbf{q}_\parallel,z) \\ F_2(\omega,\mathbf{q}_\parallel,z) \end{pmatrix}, \tag{3}$$

where the vector $\mathbf{q}_\parallel$ is the Fourier wavevector in the XY plane and $q_\parallel^2=q_x^2+q_y^2$. In equation (3) we have introduced $F_1(\omega,\mathbf{q}_\parallel,z)$ and $F_2(\omega,\mathbf{q}_\parallel,z)$ as random noise terms which are related to the Fourier transforms in time and in the XY plane of the random current tensor $\delta\hat{\mathsf{T}}(\omega,\mathbf{q}_\parallel,z)$ and of the random heat flux $\delta\hat{\mathbf{Q}}(\omega,\mathbf{q}_\parallel,z)$ in such a way that:

see equation (4) above.

The Boussinesq approximation assumes that the fluctuations in density are solely caused by temperature fluctuations. Therefore, the relationship between the temperature autocorrelation function and the dynamic structure factor, $S(\omega,\mathbf{q}_\parallel,z,z')$, is given by [11,15]:

$$\langle\theta^*(\omega,\mathbf{q}_\parallel,z)\,\theta(\omega',\mathbf{q}'_\parallel,z')\rangle = \frac{1}{\alpha^2\rho^2}S(\omega,\mathbf{q}_\parallel,z,z')\ (2\pi)^3\ \delta(\omega-\omega')\ \delta(\mathbf{q}_\parallel-\mathbf{q}'_\parallel), \tag{5}$$

where α is the cubic expansion coefficient of the liquid. For the calculation of the temperature autocorrelation function we need the correlation functions between the different components of $\delta\hat{\mathsf{T}}$ and $\delta\hat{\mathbf{Q}}$. In nonequilibrium fluctuating hydrodynamics it is assumed that, due to the existence of local equilibrium, these correlation functions will retain the same form as in equilibrium [3–5]. This assumption has been experimentally verified up to temperature gradients of 200 K cm^{-1} [26]. Fourier transforming the expressions for the real-space correlation functions of the random current tensor $\delta\mathsf{T}$ and the random heat flux $\delta\mathbf{Q}$ as, for instance, given by equations (3.12) in [4], we obtain:

$$\begin{aligned} &\langle\delta\hat{Q}_i^*(\omega,\mathbf{q}_\parallel,z)\,\delta\hat{Q}_j(\omega',\mathbf{q}'_\parallel,z')\rangle = \\ &\qquad 2k_\mathrm{B}T^2\lambda\ \delta_{ij}\ (2\pi)^3\ \delta(\omega-\omega')\ \delta(\mathbf{q}_\parallel-\mathbf{q}'_\parallel)\ \delta(z-z') \\ &\qquad \langle\delta\hat{Q}_i^*(\omega,\mathbf{q}_\parallel,z)\,\delta\hat{T}_{kl}(\omega',\mathbf{q}'_\parallel,z')\rangle = 0 \\ &\langle\delta\hat{T}_{ij}^*(\omega,\mathbf{q}_\parallel,z)\,\delta\hat{T}_{kl}(\omega',\mathbf{q}'_\parallel,z')\rangle = \\ &2k_\mathrm{B}T\eta\ (\delta_{ik}\delta_{jl}+\delta_{il}\delta_{jk})\ (2\pi)^3\ \delta(\omega-\omega')\ \delta(\mathbf{q}_\parallel-\mathbf{q}'_\parallel)\ \delta(z-z') \end{aligned} \tag{6}$$

where η is the viscosity of the liquid. Note that the equilibrium correlation functions are short ranged both in space and in time, being represented by delta functions. Consequently, the Fourier transforms, given by (6), are also proportional to delta functions in the frequency ω and in the parallel wavevector $\mathbf{q}_\parallel$.

3 Solution for two free boundaries

For the sake of completeness, we sketch here the calculation of the static structure factor for two free boundaries, as performed in [15]. This review will enable us to introduce some redefinitions which will facilitate a comparison with the calculation for two rigid boundaries to be performed in Section 4. The boundary conditions considered in [15] were:

$$\begin{aligned} \theta(\omega,\mathbf{q}_\parallel,z)&=0 \quad \text{at} \quad z=0,L \\ w(\omega,\mathbf{q}_\parallel,z)&=0 \quad \text{at} \quad z=0,L \\ \frac{\mathrm{d}^2}{\mathrm{d}z^2}\,w(\omega,\mathbf{q}_\parallel,z)&=0 \quad \text{at} \quad z=0,L, \end{aligned} \tag{7}$$

which corresponds to perfectly conducting walls and "stress-free" in the velocity. Note that these boundary conditions imply the absence of any fluctuations in the temperature and velocity of the fluid adjacent to the walls. To search for a solution of equation (3) the fluctuations $w(\omega,\mathbf{q}_\parallel,z)$ and $\theta(\omega,\mathbf{q}_\parallel,z)$ are represented as a series expansion in a complete set of eigenfunctions of the differential operator in the LHS of equation (3) satisfying the boundary conditions (7). Due to the simplicity of the boundary conditions, the appropriate set of eigenfunctions

is the Fourier sine basis in the $[0, L]$ interval [16]. We thus consider:

$$\begin{pmatrix} w(\omega, q_\parallel, z) \\ \theta(\omega, q_\parallel, z) \end{pmatrix} = \sum_{N=1}^{\infty} \begin{pmatrix} A_N(\omega, \mathbf{q}_\parallel) \\ B_N(\omega, \mathbf{q}_\parallel) \end{pmatrix} \sin\left(\frac{N\pi z}{L}\right). \quad (8)$$

To deduce the coefficients $A_N(\omega, q_\parallel)$ and $B_N(\omega, q_\parallel)$ from equation (3), we need to represent the random noise terms defined by equation (4) as a Fourier sine series, so that:

$$\begin{pmatrix} F_1(\omega, \mathbf{q}_\parallel, z) \\ F_2(\omega, \mathbf{q}_\parallel, z) \end{pmatrix} = \sum_{N=1}^{\infty} \begin{pmatrix} F_{1,N}(\omega, q_\parallel) \\ F_{2,N}(\omega, q_\parallel) \end{pmatrix} \sin\left(\frac{N\pi z}{L}\right), \quad (9)$$

where we have introduced the set of random functions $F_{1,N}(\omega, \mathbf{q}_\parallel)$ and $F_{2,N}(\omega, \mathbf{q}_\parallel)$, which are the projections onto the eigenfunction basis of the random noise terms $F_1(\omega, \mathbf{q}_\parallel, z)$ and $F_2(\omega, \mathbf{q}_\parallel, z)$. They are given by:

$$\begin{pmatrix} F_{1,N}(\omega, q_\parallel) \\ F_{2,N}(\omega, q_\parallel) \end{pmatrix} = \frac{2}{L} \int_0^L \begin{pmatrix} F_1(\omega, \mathbf{q}_\parallel, z) \\ F_2(\omega, \mathbf{q}_\parallel, z) \end{pmatrix} \sin\left(\frac{N\pi z}{L}\right) \mathrm{d}z. \quad (10)$$

Representing the random noise terms by equation (9), one readily deduces from equation (3) expressions for the coefficients of the Fourier series $A_N(\omega, q_\parallel)$ and $B_N(\omega, q_\parallel)$. The detailed expressions for these coefficients may be found in [15].

Now, to obtain the structure factor $S(\omega, q_\parallel, z, z')$ we need to evaluate the correlation functions between the projections of the random noise terms. These are readily obtained from equations (4, 10) and (6). Again the details of this calculation can be found in [15], we reproduce here the results since we shall use them below when considering "no-slip" boundary conditions:

$$\langle F^*_{1,N}(\omega, \mathbf{q}_\parallel)\, F_{1,M}(\omega', \mathbf{q}'_\parallel)\rangle =$$
$$2k_\mathrm{B}T\frac{\nu}{\rho}\frac{2}{L}\, q_\parallel^2 \left(q_\parallel^2 + \frac{N^2\pi^2}{L^2}\right)^2 \delta_{NM}\, (2\pi)^3\, \delta(\omega - \omega')\, \delta(\mathbf{q}_\parallel - \mathbf{q}'_\parallel)$$
$$\langle F^*_{1,N}(\omega, \mathbf{q}_\parallel)\, F_{2,M}(\omega', \mathbf{q}'_\parallel)\rangle =$$
$$\langle F^*_{2,N}(\omega, \mathbf{q}_\parallel)\, F_{1,M}(\omega', \mathbf{q}'_\parallel)\rangle = 0$$
$$\langle F^*_{2,N}(\omega, \mathbf{q}_\parallel)\, F_{2,M}(\omega', \mathbf{q}'_\parallel)\rangle =$$
$$\frac{2k_\mathrm{B}T^2\lambda}{\rho^2 c_P^2}\frac{2}{L}\left(q_\parallel^2 + \frac{N^2\pi^2}{L^2}\right) \delta_{NM}\, (2\pi)^3\, \delta(\omega - \omega')\, \delta(\mathbf{q}_\parallel - \mathbf{q}'_\parallel). \quad (11)$$

Note that in this calculation equation (6) is employed, which means that we have assumed that the correlation functions of the random current tensor and the random heat flux retain their local equilibrium values. This assumption remains valid as long as L is a macroscopic distance, much larger than the molecular distances in the liquid.

We have now all the information required to obtain an explicit expression for the dynamic structure factor of the fluid $S(\omega, q_\parallel, z, z')$, defined by equation (5), as a double Fourier series [15]. Integration over the frequency ω yields the static structure factor $S(q_\parallel, z, z') = (2\pi)^{-1} \int_{-\infty}^{+\infty} \mathrm{d}\omega S(\omega, q_\parallel, z, z')$. The result can be written as:

$$S(q_\parallel, z, z') = \rho^2 \kappa_T k_\mathrm{B} T \frac{\gamma - 1}{\gamma} \times \left[\delta(z - z') + \frac{(c_P/T)(\nabla T_0)^2}{D_T^2}\, \tilde{S}_\mathrm{NE}(\tilde{q}_\parallel, z, z')\right], \quad (12)$$

where $\tilde{q}_\parallel = q_\parallel L$. In equation (12) we have introduced the quantity $\tilde{S}_\mathrm{NE}(\tilde{q}_\parallel, z, z')$, which is a normalized nonequilibrium enhancement given by:

$$\tilde{S}_\mathrm{NE}(\tilde{q}_\parallel, z, z') = \frac{2L^3}{P+1} \sum_{N=1}^{\infty} \frac{\tilde{q}_\parallel^2}{(\tilde{q}_\parallel^2 + N^2\pi^2)^3} \sin\left(\frac{N\pi z}{L}\right) \sin\left(\frac{N\pi z'}{L}\right). \quad (13)$$

In deducing (12) we have made use of the thermodynamic relation: $\alpha^2 D_T = [(\gamma - 1)/\gamma]\lambda\kappa_T/T$.

In equilibrium ($\nabla T_0 = 0$), the structure factor given by equation (12) does not depend on the size of the system, L. As in the case of a bulk fluid in equilibrium the structure factor is short ranged (represented by a delta function). The fact that the equilibrium structure factor is not affected by the presence of boundaries is well known and has been already discussed in the literature, see *e.g.* [18].

The nonequilibrium contribution to the structure factor is proportional to the square of the temperature gradient $(\nabla T_0)^2$ and includes finite-size effects through the nonequilibrium contribution $\tilde{S}_\mathrm{NE}$. The dependence of $\tilde{S}_\mathrm{NE}$ on the height L was studied in [15], where the sum of the series in (13) was performed. Note that in our current definition of $\tilde{S}_\mathrm{NE}$ we have included the factor $1/(P+1)$, which makes it slightly different from the definition employed in [15]. This redefinition is more convenient for a comparison with the calculation on the basis of "no-slip" boundary conditions to be performed in Section 4. As we shall see, in the approximate calculation with "no-slip" boundary conditions the dependence on the Prandtl number cannot be collected as a prefactor in the definition of the corresponding $\tilde{S}_\mathrm{NE}$.

Several plots of $\tilde{S}_\mathrm{NE}$ for "stress-free" boundary conditions, as a function of z' for various values of z and $q_\parallel$ can be found in [15], where it is discussed how $\tilde{S}_\mathrm{NE}$ actually satisfies the boundary conditions (7). In reference [15] it is also discussed how, although the assumption of short-range correlations in the random current tensor and the random heat flux, the nonequilibrium fluctuations in real space are long-ranged, not involving any intrinsic length scale and encompassing the entire system.

4 Solution for two rigid boundaries

As in Section 3, we calculate the static structure factor of the fluid starting from the Fourier-transformed Boussinesq

equations, equation (3), supplemented with random noise terms. We continue to assume perfectly conducting walls but, contrary to Section 3, we adopt here "no-slip" boundary conditions. Thus the set of boundary conditions we shall consider in this section are:

$$\begin{aligned} \theta(\omega, \mathbf{q}_\parallel, z) &= 0 \quad \text{at} \quad z = 0, L \\ w(\omega, \mathbf{q}_\parallel, z) &= 0 \quad \text{at} \quad z = 0, L \\ \frac{\mathrm{d}}{\mathrm{d}z}\, w(\omega, \mathbf{q}_\parallel, z) &= 0 \quad \text{at} \quad z = 0, L. \end{aligned} \tag{14}$$

It is worth noting that the boundary conditions (14) are the more interesting from a experimental point of view, because they apply when a fluid layer is actually confined between two rigid solid plates [16]. The "stress-free" boundary conditions, considered in Section 3 represent a fluid confined between two free surfaces.

For "no-slip" boundary conditions, the method employed in Section 3 to calculate the static structure factor exactly is not adequate. The eigenvalues and eigenfunctions of the differential operator in the LHS of (3) satisfying the new boundary conditions (14) cannot be calculated explicitly. As discussed in [16], to calculate the eigenvalues in this case an algebraic equation is obtained which cannot be solved explicitly. The spectrum of the differential operator continues to be discrete, but the set of eigenvalues and eigenfunctions can only be calculated numerically. For this reason in the case of "no-slip" boundary conditions an explicit calculation of the structure factor can only be done approximately.

We have found that a very good approximation scheme is obtained by using a mixed Galerkin method. Thus we represent the solution for the Z-component of the velocity fluctuations as an zeroth-order Galerkin polynomial:

$$w(\omega, q_\parallel, z) = w_0(\omega, q_\parallel) \left(\frac{z}{L} - \frac{z^2}{L^2}\right)^2, \tag{15}$$

while we continue to represent the solution of the temperature fluctuations by a Fourier sine series. Note that the Galerkin polynomial we have chosen in equation (15) satisfies the required boundary conditions, given by (14). In the studies of the convective instability, the choice of the Galerkin polynomial (15) is considered to be optimal, owing to the variational structure of the underlying problem [29]. Actually, this Galerkin polynomial has been employed with excellent results to approximately calculate the critical Rayleigh number and the critical wavevector for "no-slip" boundary conditions [29].

As a standard procedure, we evaluate the amplitude $w_0(\omega, q_\parallel)$ by imposing the condition that the ansatz (15) is an exact solution for the velocity equation in the subspace generated by the Galerkin polynomial [29]. Substituting (15) in the velocity equation (3) and projecting onto the Galerkin polynomial we obtain:

$$w_0(\omega, q_\parallel) \int_0^L \left(\frac{z}{L} - \frac{z^2}{L^2}\right)^2 \left[\mathrm{i}\omega \left[\frac{\mathrm{d}^2}{\mathrm{d}z^2} - q_\parallel^2\right] - \nu \left[\frac{\mathrm{d}^2}{\mathrm{d}z^2} - q_\parallel^2\right]^2\right] \times \left(\frac{z}{L} - \frac{z^2}{L^2}\right)^2 \mathrm{d}z = G(\omega, \mathbf{q}_\parallel). \tag{16}$$

Performing the integration in (16), we get:

$$w_0(\omega, \mathbf{q}_\parallel) = \frac{-630\ L^3\ G(\omega, \mathbf{q}_\parallel)}{(\mathrm{i}\omega + \nu q_\parallel^2)\ q_\parallel^2 L^4 + 12\ (\mathrm{i}\omega + 2\nu q_\parallel^2)\ L^2 + 504\ \nu}. \tag{17}$$

In equation (16) we have introduced

$$G(\omega, \mathbf{q}_\parallel) = \int_0^L \left(\frac{z}{L} - \frac{z^2}{L^2}\right)^2 F_1(\omega, \mathbf{q}_\parallel, z)\ \mathrm{d}z. \tag{18}$$

which is the projection onto the Galerkin polynomial of the first Langevin random noise term. We use this approximate solution for $w(\omega, \mathbf{q}_\parallel, z)$ to calculate the nonequilibrium temperature fluctuations. As mentioned above, we continue to represent the temperature fluctuations by a Fourier sine series, so that:

$$\theta(\omega, \mathbf{q}_\parallel, z) = \sum_{N=1}^{\infty} B_N(\omega, \mathbf{q}_\parallel) \sin\left(\frac{N\pi z}{L}\right). \tag{19}$$

It is worth noting that if we would have used a Galerkin approximation for the temperature fluctuations, the final result, equation (25) below, would not have been proportional to a delta function when $\nabla T_0 \to 0$ and the known equilibrium structure factor would not have been recovered exactly at this limit.

To calculate the coefficients $B_N(\omega, \mathbf{q}_\parallel)$ for the temperature fluctuations we need to represent the Galerkin polynomial by a Fourier sine series:

$$\left(\frac{z}{L} - \frac{z^2}{L^2}\right)^2 = \sum_{N=1}^{\infty} W_N\ \sin\left(\frac{N\pi z}{L}\right), \tag{20}$$

where the amplitudes W_N are given by:

$$W_N = \frac{4\ (N^2\pi^2 - 12)}{N^5\pi^5}(\cos(N\pi) - 1). \tag{21}$$

Note that W_N is different from zero only for odd N. Substituting (15, 19) and (20) into the temperature fluctuations equation (3), we obtain for the coefficients $B_N(\omega, \mathbf{q}_\parallel)$:

$$B_N(\omega, \mathbf{q}_\parallel) = \frac{-W_N\ w_0(\omega, \mathbf{q}_\parallel)\ \nabla T_0 + F_{2,N}(\omega, \mathbf{q}_\parallel)}{\mathrm{i}\omega - D_T\left(\frac{N^2\pi^2}{L^2} + q_\parallel^2\right)}. \tag{22}$$

The random functions $F_{2,N}(\omega, \mathbf{q}_\parallel)$ are the projection of $F_2(\omega, \mathbf{q}_\parallel, z)$ onto the sine basis of the $[0, L]$ interval. They are the same as in the case of "free-slip" boundary conditions and were defined in equation (10).

To obtain the static structure factor of the fluid, as defined by equation (5), we need the autocorrelation function between the different projections of the Langevin random noise terms. The autocorrelations $\langle F_{2,N}^*(\omega, \mathbf{q}_\parallel)\, F_{2,M}(\omega', \mathbf{q}'_\parallel)\rangle$ were previously calculated in Section 3 and were presented in equation (11). The cross-correlations $\langle G^*(\omega, \mathbf{q}_\parallel)\, F_{2,N}(\omega', \mathbf{q}'_\parallel)\rangle$ are zero, because the

random current tensor and the random heat flux are uncorrelated (6). We now proceed to calculate the autocorrelation function of the projection onto the Galerkin polynomial of the first random noise term, $\langle G^*(\omega, \mathbf{q}_\parallel)\, G(\omega', \mathbf{q}'_\parallel)\rangle$.

Using the definition of $G(\omega, \mathbf{q}_\parallel)$, given by equation (18), the definition of $F_1(\omega, \mathbf{q}_\parallel, z)$ as a function of the Fourier transformed random current tensor, given by equation (4), and the equilibrium correlations between the different components of $\delta\hat{\mathsf{T}}(\omega, \mathbf{q}_\parallel, z)$, given by equation (6), we obtain:

$$\langle G^*(\omega, \mathbf{q}_\parallel) \cdot G(\omega', \mathbf{q}'_\parallel)\rangle = 2k_\mathrm{B}T\frac{\nu}{\rho}\, q_\parallel^2\, (2\pi)^3 \times \delta(\omega-\omega')\, \delta(\mathbf{q}_\parallel - \mathbf{q}'_\parallel) \int_0^L\int_0^L \left(\frac{z}{L}-\frac{z^2}{L^2}\right)^2 \left(\frac{z'}{L}-\frac{z'^2}{L^2}\right)^2 \times \left[q_\parallel^4 + q_\parallel^2\left(\frac{\mathrm{d}^2}{\mathrm{d}z^2}+\frac{\mathrm{d}^2}{\mathrm{d}z'^2}+4\frac{\mathrm{d}}{\mathrm{d}z}\frac{\mathrm{d}}{\mathrm{d}z'}\right)+\frac{\mathrm{d}^2}{\mathrm{d}z^2}\frac{\mathrm{d}^2}{\mathrm{d}z'^2}\right] \times \delta(z-z')\, \mathrm{d}z\, \mathrm{d}z'. \quad (23)$$

Now we integrate by parts the different terms of equation (23), to move the differential operator inside the double integral from the delta function to the Galerkin polynomials preceding it. Note that since in all cases an even number of integrations are required, there will not be any change of sign in the process. With this procedure, the integration yields:

$$\langle G^*(\omega, \mathbf{q}_\parallel)\cdot G(\omega', \mathbf{q}'_\parallel)\rangle = 2k_\mathrm{B}T\frac{\nu}{\rho}\, q_\parallel^2\, \frac{q_\parallel^4 L^4 + 24\, q_\parallel^2 L^2 + 504}{630 L^3} \times (2\pi)^3\, \delta(\omega-\omega')\, \delta(\mathbf{q}_\parallel - \mathbf{q}'_\parallel), \quad (24)$$

which is the autocorrelation function we were trying to calculate. Now we have all the required information to obtain the dynamic structure factor of the fluid, $S(\omega, \mathbf{q}_\parallel, z, z')$. As before, integration over the frequency ω gives the static structure factor. We find just as for "stress-free" boundary conditions, that the static structure factor can be written as:

$$S(q_\parallel, z, z') = \rho^2\kappa_T k_\mathrm{B}T\frac{\gamma-1}{\gamma} \times \left[\delta(z-z') + \frac{(c_P/T)(\nabla T_0)^2}{D_T^2}\, \tilde{S}_\mathrm{NE}(\tilde{q}_\parallel, z, z')\right], \quad (25)$$

where again $\tilde{q}_\parallel = q_\parallel L$. Note that equation (25) for "no-slip" boundary conditions is exactly the same as equation (12) for "stress-free" boundary conditions. But in the "no-slip" case the expression for the normalized nonequilibrium enhancement, $\tilde{S}_\mathrm{NE}(\tilde{q}_\parallel, z, z')$, is more complicated, being:

$$\tilde{S}_\mathrm{NE}(\tilde{q}_\parallel, z, z') = L^3\, \frac{630\, \tilde{q}_\parallel^2}{\tilde{q}_\parallel^2 + 12} \times \sum_{N=1}^{\infty}\sum_{M=1}^{\infty}\left\{\frac{1}{N^2\pi^2 + \tilde{A}(P, \tilde{q}_\parallel)} + \frac{1}{M^2\pi^2 + \tilde{A}(P, \tilde{q}_\parallel)}\right\} \times \frac{W_M W_N}{(N^2+M^2)\pi^2 + 2\tilde{q}_\parallel^2} \sin\left(\frac{N\pi z}{L}\right)\, \sin\left(\frac{M\pi z'}{L}\right), \quad (26)$$

where we have introduced a dimensionless function $\tilde{A}(P, \tilde{q}_\parallel)$, defined by:

$$\tilde{A}(P, \tilde{q}_\parallel) = \tilde{q}_\parallel^2 + P\, \frac{(\tilde{q}_\parallel^2 + 12)^2 + 360}{(\tilde{q}_\parallel^2 + 12)}\,. \quad (27)$$

This new parameter $\tilde{A}$ arises from the integration in the frequencies ω included in the calculation. It is worth mentioning that, in the zeroth-order Galerkin approximation we have used, $\tilde{S}_\mathrm{NE}$ depends on the Prandtl number through $\tilde{A}(P, q_\parallel L)$. Thus, contrary to the case of "stress-free" boundary conditions, the dependence on P can no longer be collected as a prefactor in the definition of $\tilde{S}_\mathrm{NE}$. On the other hand, we note that due to the cylindrical symmetry of the problem the result depends only on the magnitude $q_\parallel$ of the vector $\mathbf{q}_\parallel$.

In equilibrium ($\nabla T_0 = 0$) we obtain from equation (25) the same result obtained previously in Section 3 for "stress-free" boundary conditions which is the well known short-range correlation function for a fluid in equilibrium [4], $S_\mathrm{E} = \rho^2\kappa_T k_\mathrm{B}T[(\gamma-1)/\gamma]$. Again the equilibrium structure factor is not affected by the presence of boundaries. However, contrary to the case of "stress-free" boundary conditions, the double Fourier series representing $\tilde{S}_\mathrm{NE}$ for "no-slip" boundary conditions, equation (26), contains cross terms and the sum cannot be performed explicitly.

To compare our results for two rigid boundaries with those obtained for two free boundaries, we have plotted in Figure 1, as a dashed line, the exact $L^{-3}\tilde{S}_\mathrm{NE}(q_\parallel, z, z')$ for two free boundaries, given by equation (13). We have also plotted in Figure 1, as a solid line, the zeroth-order Galerkin approximation to $L^{-3}\tilde{S}_\mathrm{NE}(q_\parallel, z, z')$ for two rigid boundaries, given by equation (26). In both cases $L^{-3}\tilde{S}_\mathrm{NE}(q_\parallel, z, z')$ is plotted as a function of z'/L, for $z = L/2$, $q_\parallel = 22/L$, and for the case that $P = 8$, which is close to the value corresponding to pure toluene at 25 °C.

Figure 1 shows that, in both cases, $L^{-3}\tilde{S}_\mathrm{NE}(q_\parallel, z, z')$ is a function peaked at $z = z'$ and, as a consequence of the perfectly conducting walls assumption, it goes to zero at both ends of the $[0, L]$ interval. Comparing the two plots in Figure 1 we observe that, for the same value of $q_\parallel$, the peak at $z = z'$ is broader and lower in the case of two rigid boundaries. It is difficult to conclude whether this behavior is a consequence of the Galerkin approximation used for "no-slip" boundary conditions. Anyway this difference is congruent with the well known fact that "no-slip" boundary conditions are more stabilizing: the critical Rayleigh number and the critical wavevector are larger for "no-slip" than for "stress-free" boundary conditions.

5 Consequences for light-scattering experiments

The quantity that is actually measured in a light-scattering experiment is the intensity of the scattered light as a function of the scattering angle. We

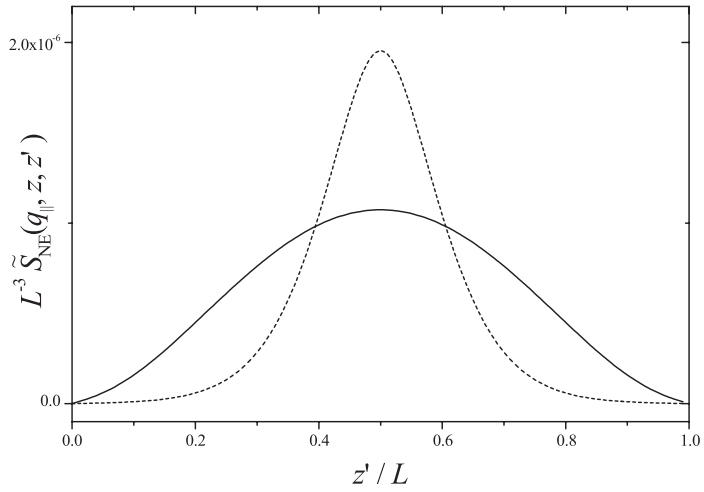

Fig. 1. Normalized nonequilibrium enhancement $L^{-3}\tilde{S}_{\rm NE}(q_\parallel, z, z')$ of the static structure factor as a function of z'/L for $z/L = L/2$ and $q_\parallel = 22/L$. The solid line is for two rigid boundaries while the dashed line is for two free boundaries. In both cases the Prandtl number is $P = 8$.

are considering here low-angle light-scattering experiments like the ones performed by Sengers and coworkers at Maryland [8–10,26] or by Vailati and Giglio at Milan [13,14]. An schematic representation of such experiments is shown in Figure 2. The scattering medium is a thin horizontal fluid layer bounded by two parallel plates whose temperatures can be controlled independently so as to establish a temperature gradient across the fluid layer. The boundary plates are furnished with windows allowing laser light to propagate through the fluid in the direction (anti)parallel to the temperature gradient. Light scattered over an angle ϕ arises from fluctuations with wave number such that:

$$q = 2\, q_0 \sin(\phi/2), \tag{28}$$

where q_0 is the wave number of the incident light inside the scattering medium. To observe the nonequilibrium enhancement in the scattered intensity one needs to measure the intensity of the scattered light at small wave numbers and, hence, at very small scattering angles.

From electromagnetic theory it follows that the scattering intensity $S(\mathbf{q})$ is obtained from an integration of the structure factor over the scattering volume, so that [4,15]:

$$S(q_\parallel, q_\perp) = \frac{1}{L}\int_0^L \int_0^L \mathrm{e}^{-\mathrm{i}q_\perp(z-z')} S(q_\parallel, z, z')\, \mathrm{d}z\mathrm{d}z'. \tag{29}$$

In (29) we have assumed that the scattering volume extends over the full height of the fluid layer, as is the case in small-angle light-scattering from very thin fluid layers. In this situation scattered light received in the collecting pinhole of the detector indeed originates from all points illuminated by the laser beam inside the fluid layer. Note that the experimental arrangement we are considering has cylindrical symmetry so the scattered-light intensity will only depend on the magnitudes $q_\parallel$ and $q_\perp$ of the scattering wavevector $\mathbf{q}$. In addition, in an actual light-scattering

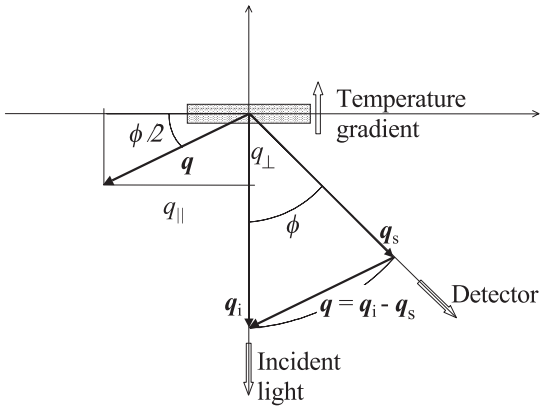

Fig. 2. Schematic representation of a typical experimental arrangement employed in low-angle light-scattering experiments.

experiment, $q_\parallel$ and $q_\perp$ are not independent variables, because they are related by the geometry of the experiment, represented in Figure 2, and by the Bragg condition (28), see also [15].

The goal of the present section is to compare the scattering light intensity $S(q_\parallel, q_\perp)$ obtained for free boundaries and for rigid boundaries. In the case of two free boundaries $S(q_\parallel, q_\perp)$ can be calculated by substituting equations (12) and (13) in equation (29) and by performing the summation in equation (13) and the integration in equation (29). This calculation can be done exactly, the result being a complicated function of $q_\parallel$ and $q_\perp$ [15]. In the case of two rigid boundaries, $S(q_\parallel, q_\perp)$ can be calculated by substituting equations (25) and (26) in equation (29) and by performing the integration in equation (29). In this case the summation in (26) cannot be performed explicitly. Nevertheless, due to the similar structure of equation (12) for free boundaries and equation (25) for rigid boundaries,

in both cases the scattered light intensity can be separated into an equilibrium contribution $S_{\rm E}$ and a nonequilibrium enhancement, $\tilde{S}_{\rm NE}(q_\parallel, q_\perp)$, such that:

$$S(q_\parallel, q_\perp) = S_{\rm E}\left[1 + \frac{(c_P/T)(\nabla T_0)^2}{D_T^2}\ \tilde{S}_{\rm NE}(q_\parallel, q_\perp)\right]. \quad (30)$$

The equilibrium contribution is the result obtained when $\nabla\ T_0 = 0$, which in both cases is isotropic (independent of the wavevector $\mathbf{q}$) and is expressed as:

$$S_{\rm E} = \rho^2 \kappa_T k_{\rm B} T \frac{\gamma - 1}{\gamma}\,. \quad (31)$$

Equation (31) is the traditional formula for the equilibrium isotropic Rayleigh-scattering intensity [7]. Hence the boundary conditions ("stress-free" or "no-slip") do not affect the Rayleigh scattering from a liquid in thermal equilibrium. This result remains valid as long as the height of the liquid layer L is large enough so that the correlation functions for the random noise terms retain their equilibrium values given by equation (6).

The calculation of the nonequilibrium enhancement for "stress-free" boundary conditions performed in [15] can be substantially simplified if we assume that the scattering angles are so small that $q_\parallel \simeq q$ and $q_\perp \simeq 0$. In such a case the nonequilibrium enhancement is readily expressed as a function of only the magnitude of the wavevector q. It is interesting to note that nonequilibrium fluctuations have been also observed by the shadowgraph technique [30,31]. The quantity actually measured in these experiments is $S(q_\parallel = q, q_\perp = 0)$, where q is the magnitude of a two dimensional Fourier vector in the imaging plane of the shadowgraph [32]. Consequently the case $q_\parallel = q$ and $q_\perp = 0$ is the most interesting from an experimental point of view. For "stress-free" boundary conditions, substituting equation (13) into equation (29) we have earlier obtained for this particular case [15]:

$$\tilde{S}_{\rm NE}(\tilde{q}) = \frac{L^4}{(P+1)\ \tilde{q}^4} \times \left\{1 + \frac{\tilde{q}^2[\cosh(\tilde{q}) - 1] + \sinh(\tilde{q})[7\tilde{q} - 15\sinh(\tilde{q})]}{4\tilde{q}\sinh(\tilde{q})[\cosh(\tilde{q}) + 1]}\right\}, \quad (32)$$

where $\tilde{q} = qL$. For nonequilibrium light-scattering, equation (32) is valid up to order $\sin^2(\phi/2)$ in terms of the scattering angle ϕ. In actual experiments the angles are so small that equation (32) is an excellent approximation indeed [15].

In the case of "no-slip" boundary conditions, substituting equation (26) into equation (29) and performing the integration, we obtain:

$$\tilde{S}_{\rm NE}(\tilde{q}) = \frac{5040\ L^2\tilde{q}^2}{\pi^2\ (\tilde{q}^2 + 12)} \times \sum_{N=1}^{\infty}\sum_{M=1}^{\infty} \frac{1}{N^2\pi^2 + \tilde{A}(P,\tilde{q})} \times \frac{1}{(N^2+M^2)\pi^2 + 2\tilde{q}^2} \frac{W_N W_M}{N\ M}, \quad (33)$$

where the function $\tilde{A}(P, \tilde{q}_\parallel)$ was defined by equation (26). As before, we have not been able to sum the series in equation (33), and we cannot obtain a more compact expression.

It is interesting to study the nonequilibrium enhancement in the limits $\tilde{q} \to 0$ and $\tilde{q} \to \infty$. The case of "stress-free" boundary conditions was already considered in reference [15]. From equation (32) it can be readily shown that:

$$\tilde{S}_{\rm NE}(\tilde{q}) \xrightarrow{\tilde{q}\to 0} \frac{17}{20160}\ \frac{L^4}{P+1}\ \tilde{q}^2, \quad (34)$$

and

$$\tilde{S}_{\rm NE}(\tilde{q}) \xrightarrow{\tilde{q}\to \infty} \frac{L^4}{P+1}\ \frac{1}{\tilde{q}^4}\,. \quad (35)$$

The case of "no-slip" boundary conditions is considered for the first time in the present paper. From equation (33) we obtain the asymptotic behaviors:

$$\tilde{S}_{\rm NE}(\tilde{q}) \xrightarrow{\tilde{q}\to 0} \frac{420\ L^4}{\pi^4}\ \tilde{F}(P)\ \tilde{q}^2, \quad (36)$$

and

$$\tilde{S}_{\rm NE}(\tilde{q}) \xrightarrow{\tilde{q}\to \infty} \frac{7}{10}\ \frac{L^4}{P+1}\ \frac{1}{\tilde{q}^4}, \quad (37)$$

where in equation (36) we have introduced the dimensionless function $\tilde{F}(P)$ of the Prandtl number P, given by:

$$\tilde{F}(P) = \sum_{N=1}^{\infty}\sum_{M=1}^{\infty} \frac{W_N W_M}{(N^2+M^2)(N^2\pi^2 + 42P)NM}\,.$$

From equations (34–37) we conclude that for the case of "stress-free" and for the case of "no-slip" boundary conditions we have the same qualitative behavior. The typical q^{-4} divergence in the nonequilibrium enhancement of the structure factor crosses over to a q^2 dependence for extremely small q values as a consequence of the finite-size of the system. In the case of "stress-free" boundary conditions, in the limit $q \to \infty$ we recover the "bulk" result, obtained when no boundary conditions are taken into account, as is evident from a comparison of equations (30) and (35) with equation (1). Note that large values of q correspond to fluctuations with a very short length scale, for which finite-size effects are expected to be of no influence. For the case of "no-slip" boundary conditions we recover the expected "bulk" result only qualitatively, but quantitatively we are 30% short. This shortcoming is a consequence of the fact that for "no-slip" boundary conditions our calculation is only approximate. If higher-order terms in the Galerkin approximation are considered we shall gradually approach the correct result. Indeed, we have performed a first-order Galerkin calculation and we have found that when first-order corrections are included, the numerical prefactor in equation (37) increases from 0.7 to 0.857, thus approaching the "bulk" solution as expected. We are not

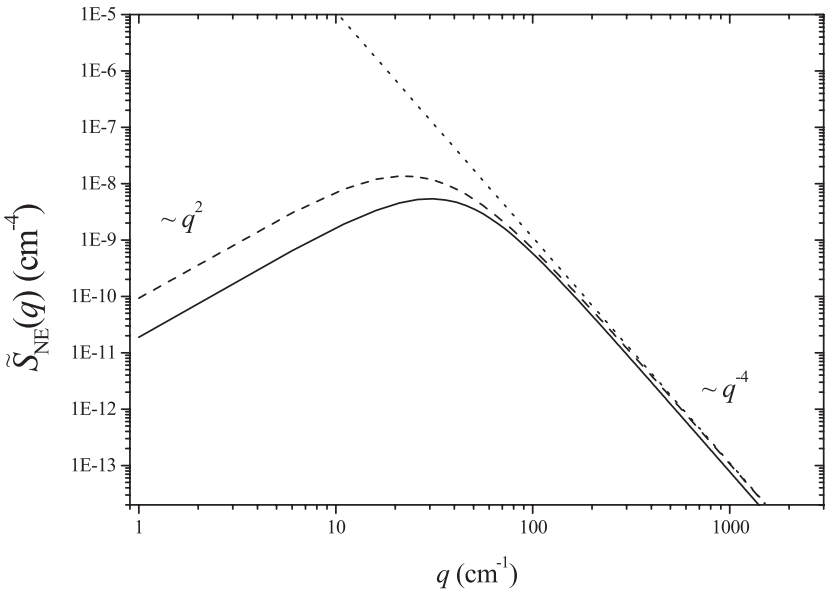

Fig. 3. Double-log plot of the normalized nonequilibrium enhancement $\tilde{S}_{\rm NE}(q)$ of the static structure factor as a function of the scattering wavevector q. The solid line is the approximate result for two rigid boundaries, the dashed line is the exact result for two free boundaries, and the dotted line represents the exact "bulk" result, with no boundary conditions taken into account. For the three cases, $P = 8$. For the two finite-size cases, $L = 0.1$ cm.

giving the details of this calculation here, but just mention that the first-order Galerkin approximation we used was: $(z/L - z^2/L^2)^2\ [w_0(\omega, q_\parallel) + w_1(\omega, q_\parallel)\ (1/2 - z/L)]$.

To compare the results with free and with rigid boundaries we have plotted in Figure 3, as a dashed line, the exact $\tilde{S}_{\rm NE}(q)$ for "stress-free" boundary conditions given by equation (32). We have also plotted in Figure 3, as a solid line, the first-order Galerkin approximation to $\tilde{S}_{\rm NE}(q)$ for "no-slip" boundary conditions given by equation (33). For completeness we have also plotted in Figure 3, as a dotted line, the "bulk" result, given by (35), which is obtained without taking into account boundary conditions. In the three cases the scattering angles are assumed to be small, thus $q_\parallel \simeq q$ and $q_\perp \simeq 0$. A double logarithmic scale is used. For the Prandtl number we have adopted the value $P = 8$, which is close to the value for pure toluene at 25 °C. For the "stress-free" and for the "no-slip" cases we took $L = 0.1$ cm, which is a typical height of fluid layers in nonequilibrium Rayleigh-scattering experiments.

A simple inspection of Figure 3 confirms that finite-size effects cause the q^{-4} divergence to cross over to a q^2 dependence for extremely small wavevectors q, as implied by the equations discussed earlier. There appears a maximum separating both behaviors, indicating that the enhancement of the fluctuations is largest for a particular wavevector $q_{\rm max}$. The wavevector corresponding to the maximum intensity is of the order of the inverse of the height of the cell $q_{\rm max} \simeq 1/L$. Numerically we find that, for two free boundaries the maximum appears at $q_{\rm max} = 2.222/L$, while for two rigid boundaries the position of the maximum depends on the Prandtl number. For $P = 8$, which is the value employed in Figure 3, we found $q_{\rm max} = 3.032/L$. It is worth remembering that the calculation performed in the latter case is only a zeroth-order approximation. If higher-order terms are accounted for, $q_{\rm max}$ will shift. In any case, the length scale corresponding to $q_{\rm max}$ is macroscopic.

From Figure 3 one can also see that the "stress-free" curve has the correct asymptotic behavior for large q because it approaches the "bulk" solution, whereas the "no-slip" curve remains a bit below. As discussed before, this is a consequence of the fact that the "no-slip" curve shown in Figure 3 is only the zeroth-order Galerkin approximation.

Another feature that can be observed in Figure 3 is that the maximum for the "no-slip" curve is lower and displaced to higher wavevectors, when compared with the maximum for the "stress-free" curve. This result is consistent with the well-known fact that "no-slip" boundary conditions are more stabilizing: the convective instability appears at larger Rayleigh numbers and larger wavevectors [16]. Again, and as at the end of Section 4, it is difficult to conclude whether this effect is real or is an artifact resulting from the approximation in the calculation for "no-slip" boundary conditions. As already mentioned, we performed a first-order Galerkin approximation. It turns out that the effect of first-order terms on the position and the height of the maximum is very small and the $q_{\rm max}$ and the height of the maximum for the "no-slip" curve continue to be larger when compared with the "stress-free" curve.

Since we neglect the buoyancy term in the Boussinesq equations, gravity effects have not been taken into account in the present work. If they would be included, we expect that for positive Rayleigh number, as the convective instability is approached, the maximum in $S(q)$ will

become larger and larger. Fluctuations with $q \simeq 1/L$ are expected to be more and more enhanced. At the critical Rayleigh number the value of $S(q)$ at $q_{\max}$ should diverge as $(R_c - R)^{-1}$, as is discussed in various publications studying the influence of thermal noise close to the convective instability [17–21]. This divergence has been observed experimentally by the shadowgraph technique [30]. For negative Rayleigh numbers, as mentioned in the Introduction, gravity has a damping effect on nonequilibrium fluctuations making the q^{-4} divergence of $\tilde{S}_{NE}$ to reach a constant limit when $q \to 0$ [11,13]. The gravitationally induced saturation of the q^{-4} divergence occurs at a "roll-off" wave number q_{RO} such that [11,13]:

$$q_{RO} = \left(\frac{g\alpha \nabla T_0}{\nu D_T} \right)^{1/4} \tag{38}$$

where g is the gravitational acceleration constant. For pure toluene subjected to a temperature gradient $\nabla T_0 = 100$ K cm^{-1} we find $q_{RO} = 70$ cm^{-1} [8,11]. From Figure 3 we note that at this wave number deviations from the q^{-4} behavior due to finite-size effects are substantial. Thus we conclude that, at least in one-component liquids, finite-size effects may be equally important as deviations from the q^{-4} behavior due to gravity.

6 Conclusions

In this paper we have calculated the static structure factor of a fluid from the linearized random Boussinesq equations using the realistic "no-slip" boundary conditions and neglecting gravity effects. The calculation was performed by using a zeroth-order Galerkin approximation for the solution of the fluctuating velocity equation. The consequences for low-angle light-scattering experiments have been elucidated.

The result obtained here for two rigid boundaries has qualitatively the same behavior as that from an exact calculation performed earlier for two free boundaries [15]. The typical q^{-4} divergence of the nonequilibrium structure factor crosses over to a q^2 dependence for extremely small scattering angles. Separating both behaviors there is a maximum in the scattered intensity, indicating that fluctuations with a particular wavevector, $q_{\max}$, are maximally enhanced. The value of $q_{\max}$ depends on the boundary conditions considered, but in any case, it is of the order of the inverse of the height of the fluid layer $q_{\max} \simeq 1/L$. This fact indicates that, even below the conductive instability, fluctuating structures do appear in the system. Above the convective threshold these fluctuating structures will develop convection rolls.

Our present work shows how the nonequilibrium conditions combined with the finite-size of the system cause the selection of a particular length scale in the system, thus giving a nonequilibrium finite-size system the ability to develop spatially extended patterns. While patterns can be macroscopically visualized only above the convective threshold, they could be investigated, *below* the convective threshold, by ultra-low-angle light-scattering experiments.

We are indebted to M. Rubí and A.L. Garcia for suggestions and comments. We particularly acknowledge J.V. Sengers for constant encouragement and careful reviewing of our manuscript, without his invaluable help, this work would not have been completed.

References

1. J.R. Dorfman, T.R. Kirkpatrick, J.V. Sengers, Annu. Rev. Phys. Chem. **45**, 213 (1994).
2. T.R. Kirkpatrick, E.G.D. Cohen, J.R. Dorfman, Phys. Rev. A **26**, 995 (1982).
3. D. Ronis, I. Procaccia, Phys. Rev. A **26**, 1812 (1982).
4. R. Schmitz, E.G.D. Cohen, J. Stat. Phys. **40**, 431 (1985).
5. R. Schmitz, Phys. Rep. **171**, 1 (1988).
6. B.M. Law, J.V. Sengers, J. Stat. Phys. **57**, 531 (1989).
7. B.J. Berne, R. Pecora, *Dynamic Light Scattering* (Wiley, New York, 1976).
8. B.M. Law, P.N. Segrè, R.W. Gammon, J.V. Sengers, Phys. Rev. A **41**, 816 (1990).
9. W.B. Li, P.N. Segrè, R.W. Gammon, J.V. Sengers, Physica A **204**, 399 (1994).
10. W.B. Li, K.J. Zhang, J.V. Sengers, R.W. Gammon, J.M. Ortiz de Zárate, Phys. Rev. Lett. **81**, 5580 (1998).
11. P.N. Segrè, R. Schmitz, J.V. Sengers, Physica A **195**, 31 (1993).
12. P.N. Segrè, J.V. Sengers, Physica A **198**, 46 (1993).
13. A. Vailati, M. Giglio, Phys. Rev. Lett. **77**, 1484 (1996).
14. A. Vailati, M. Giglio, Prog. Colloid. Polym. Sci. **104**, 76 (1997).
15. J.M. Ortiz de Zárate, R. Pérez Cordón, J.V. Sengers, Physica A **291**, 113 (2001).
16. Chandrasekhar, *Hydrodynamic and Hydromagnetic Instability* (Clarendon, Oxford, 1961).
17. J.B. Swift, P.C. Hohenberg, Phys. Rev. A **15**, 319 (1977).
18. T.R. Kirkpatrick, E.G.D. Cohen, J. Stat. Phys. **33**, 639 (1983).
19. R. Schimtz, E.G.D. Cohen, J. Stat. Phys. **39**, 285 (1985).
20. H. van Beijeren, E.G.D. Cohen, J. Stat. Phys. **53**, 77 (1988).
21. P.C. Hohenberg, J.B. Swift, Phys. Rev. A **46**, 4773 (1992).
22. M. Malek Mansour, J.W. Turner, A.L. García, J. Stat. Phys. **48**, 1157 (1987).
23. M. Malek Mansour, A.L. García, J.W. Turner, M. Mareschal, J. Stat. Phys. **48**, 295 (1987).
24. I. Bena, M. Malek Mansour, G.C. Lie, E. Clementi, Phys. Rev. E **59**, 5503 (1999).
25. M.C. Cross, P.C. Hohenberg, Rev. Mod. Phys. **65**, 851 (1993).
26. P.N. Segrè, R.W. Gammon, J.V. Sengers, B.M. Law, Phys. Rev. A **45**, 714 (1992).
27. L.D. Landau, E.M. Lifshitz, *Fluid Mechanics* (Addison-Wesley, Reading MA, 1959).
28. D. Ronis, I. Procaccia, J. Machta, Phys. Rev. A **22**, 714 (1980).
29. P. Manneville, *Dissipative Structures and Weak Turbulence* (Academic Press, San Diego 1990) p. 109.
30. M. Wu, G. Ahlers, D.S. Cannell, Phys. Rev. Lett. **75**, 1743 (1995).
31. D. Brogioli, A. Vailati, M. Giglio, Phys. Rev. E **61**, R1 (2000).
32. J.R. de Bruyn, E. Bodenschatz, S.W. Morris, S.P. Trainoff, Y. Wu, D.S. Cannell, G. Ahlers, Rev. Sci. Instrum. **67**, 2043 (1996).